Selective-correlation velocity analysis

Valmore Celis and Ken Larner
Center for Wave Phenomena, Department of Geophysics, Colorado School of Mines, Golden, CO 80401-1887

ABSTRACT
Resolution in velocity spectra depends primarily on cable length, reflector depth, stacking velocity, and dominant frequency of the data. Velocity spectra often fail to separate interfering events, particularly (but not exclusively) those at late times and with high velocities. The need for increased resolution in velocity spectra is clear when one wishes to distinguish between two neighboring primary events from reflectors with conflicting dip, or to identify weak primaries in the presence of strong multiples.
Velocity-spectrum methods transform data from the offset and reflection-time domain to the stacking velocity and zero-offset, two-way traveltime domain. This transformation can be achieved using any of several coherence measures based on the crosscorrelation of the traces; the more commonly used are semblance coefficient, unnormalized crosscorrelation sum, and statistically normalized crosscorrelation sum. All these measures involve crosscorrelations between traces in a collection such as a common-midpoint (CMP) gather or common-image gather (CIG). One might think that, for a given number of data traces, the sum of all possible crosscorrelations should be a more reliable measure than the sum of only a subset of the crosscorrelations. We show, however, that use of selected subsets of crosscorrelations can improve both the reliability and resolution of velocity analysis. Such subsets are formed by including in the summation only those crosscorrelations for whose pair of traces the relative differential moveout of reflections exceeds some threshold established *a priori,* and discarding those crosscorrelations for which the associated differential moveout is relatively small. We have called this process *selective-correlation* velocity analysis.
Comparisons of the performances on a variety of synthetic model data show that selective-correlation velocity analysis considerably enhances the resolving power of velocity spectra over that of conventional crosscorrelation sum in the presence of statics distortions and random noise, at no sacrifice in the quality of results. For closely interfering reflections under these perturbing conditions, selective-correlation velocity analysis retains its greater resolution power. Moreover, this improvement in performance is achieved at computational cost that is comparable to that for conventional velocity analysis.

Key words: velocity analysis, resolution

Introduction

The standard approach for estimating stacking velocities is to pick maxima in some coherence measure at fixed zero-offset reflection times (Taner and Koehler, 1969). For a given CMP gather, the velocity spectrum at a given time is computed by fixing a reference time $t_{0,i}$, and then sweeping over a predetermined set of trial velocities $(v_1, v_2, ..., v_n)$, usually at a regular interval Δv. Each pair of $t_{0,i}$ and v_m will produce a particular hyperbolic moveout pattern. Then, the velocity spectrum, for fixed time $t_{0,i}$, is obtained by a correlation process along each of those hyperbolas. A peak in the spectrum indicates the velocity corresponding to a hyperbolic move-

out that fits the data relatively well. This procedure is repeated for different uniformly incremented times ($t_{0,1}, t_{0,2}, \ldots$) either until the end of the record or a specified maximum time is reached. The computed velocity spectra for all normal-incidence times $t_{0,i}$ is displayed as a function of zero-offset traveltime and trial velocity. Then, the picking process begins. Our interest here, however, is focused solely on the spectra computation.

Several good properties of stacking-velocity spectra can be mentioned: (1) they provide maximum-likelihood estimates for stacking velocity of well-separated reflections in the presence of additive uncorrelated noise with Gaussian statistics, (2) they are robust with respect to deviations of the noise from being Gaussian, (3) implementation is relatively simple and computationally much less intensive than, for example, eigenvalue methods (e.g., Biondi and Kostov, 1989; Key and Smithson, 1990), and (4) when two or more events have close arrival times at zero offset but their corresponding moveouts are sufficiently different, conventional velocity spectra produces good estimates of primary stacking velocity. When, however, a pair of events are too close to one another and have little moveout difference, relative to the dominant period in the data, the estimates can biased and, even worse, the spectra may show only one (erroneous) maximum for a given $t_{0,i}$.

Resolution in velocity spectra depends primarily on cable length, depth of the reflecting interface, overburden velocity (more specifically, stacking velocity), and dominant frequency of the data. Stacking-velocity spectra often fail to separate interfering events at late times and high velocities, and even relatively shallow events that are dominated by low frequencies and have relatively small moveout difference. The need for high-resolution velocity spectra is clear when one wishes to distinguish two neighboring primary events coming from reflectors with conflicting dip, or to identify weak primaries in the presence of strong multiples.

De Vries and Berkhout (1984) addressed the resolution problem using a tool for velocity analysis based on minimum entropy. This approach analyzes the spectral content of data as a function of moveout parameters such as stacking velocity for a CMP gather and migration velocity for a common-image gather (CIG). To obtain an estimate of the stacking velocity using minimum entropy velocity analysis, however, one must specify a window around the zero-offset time of a targeted reflection.

Gelchinsky et al. (1985) considered algorithms of phase and group correlation based on different assumptions about the wavefield. These correlation algorithms require the construction of functionals that must be analyzed in order to estimate the parameters (e.g., velocity) of the detected signal. Such analysis is performed using a system of inequalities that depend on parameters whose determination and influence on velocity analysis is unclear. Another resolution-enhancement method for seismic velocity analysis, based on the eigenstructure decomposition of the covariance matrix of the data, was developed by Biondi and Kostov (1989). Their method can be powerful in resolving closely interfering reflections; unlike conventional velocity spectra, however, the number of events in conflict must be estimated *a priori* at each time level, which is impractical for field data. Furthermore, the influence of noise in data on their method is not well understood, and the method is computationally more costly than other commonly-used velocity-analysis methods.

A convenient alternative approach to increase resolution in conventional velocity analysis is through use of optimum weights for traces that are to be CMP stacked. Schoenberger (1996) described a method for multiple suppression, called *optimum weighted stack*, that requires knowledge of the differential moveout between a targeted multiple and primary, along with the frequency content of the multiple. The weights produced in Schoenberger's method can be used to improve velocity resolution by applying them directly to the traces in the CMP gather prior to performing velocity analysis.

Several other authors have dealt with the problem of optimizing the velocity-estimation process or improving the resolution of stacking velocity analysis (e.g., Kirling et al., 1984; Toldi, 1989). Each of these methods has relative advantages and limitations: where one method fails, another may succeed, and vice versa. As a result, tradeoffs have to be made, for instance between resolution and robustness.

Here, we present a method for increasing the resolution of stacking velocity analysis that allows the analyst to distinguish more clearly between primary and multiple reflections, or between neighboring primary events, than with conventional velocity analysis. This approach preserves the good properties of conventional velocity analysis, while introducing only a relatively minor modification (at comparable computation effort) to conventional velocity-spectra calculation.

Approach

The methodology for this work is based on the sum of crosscorrelations described by Neidell and Taner (1971). They described both normalized and unnormalized coherence measures; our method can be applied using either. Here, we describe the approach in terms of the unnormalized crosscorrelation measure (UC) given, as a function of trial velocity v_{trial} and two-way zero-offset traveltime t_0, by

$$UC(v_{trial}, t_0) = \sum_{k=1}^{M-1} \sum_{j=k+1}^{M} \sum_{w} f_{k,t(k)}\ f_{j,t(j)}, \qquad (1)$$

where M is the number of traces in the CMP gather, $f_{j,t(j)}$ is the amplitude on the jth trace along a reflection-time trajectory $t(j)$, and w is a specified time

window centered on that trajectory. In stacking-velocity estimation, this trajectory $t(j)$ is the reflection time along a hyperbola governed by a trial velocity v_{trial},

$$t(j) = \sqrt{t_0^2 + \frac{x_j^2}{v_{trial}^2}}, \tag{2}$$

where x_j is the offset from the source to detector j and t_0 is the two-way zero-offset traveltime at the center of the time window. Because the time window w is symmetrically placed around the reflection-time hyperbola $t(j)$ for the jth trace, the boundaries of the time window w are parallel to hyperbolic trajectory (2) over the entire spreadlength.

In the approach of Neidell and Taner, all possible crosscorrelations among the traces of a CMP gather are summed, giving the same weight to each contributing correlation independent of the differential moveout between crosscorrelated traces. If the differential moveout is small, however, as occurs especially for short-offset traces, reflection events on the traces will be approximately in phase for a relatively wide range of velocities, giving a broad semblance response as a function of trial velocity (Sherwood and Poe, 1972). In contrast, crosscorrelation of a pair of traces with large differential moveout offers relatively larger resolving power for the velocity estimation. The core idea behind the approach here is thus to allow into the summation only those crosscorrelations whose pair of traces have a relatively large differential moveout. To achieve this goal, we use a *selective crosscorrelation sum* that excludes correlations of pairs of traces from the spectrum computation based on differential moveout of reflections.

In order to do the selection, a numerical *significance* value is first assigned to each pair of crosscorrelated traces using a parabolic trajectory as a convenient approximation of moveout. For the source-to-receiver offsets x_j and x_k on the jth and kth traces, with $j > k$, the parabolic approximation of the differential moveout Δt_{jk} is proportional to the difference of squared offsets,

$$\Delta t_{jk} \propto x_j^2 - x_k^2, \tag{3}$$

and the significance value is defined as

$$S_{jk} = \frac{x_j^2 - x_k^2}{x_{\max}^2 - x_0^2}, \tag{4}$$

where $x_{\max}$ is the maximum offset, and x_0 the minimum offset. Each possible crosscorrelation pair is thus assigned a significance value, which by equation (4) is normalized over the range zero to one. The *autocorrelation* of any given trace clearly has no significance for estimation of stacking velocity because the differential moveout for a trace and itself is zero. A significance value of unity is associated with the maximum differential moveout possible, and thus with the crosscorrelation between traces for the shortest and the longest offsets.

We then specify a threshold for these significance values; all crosscorrelations with significance values below this threshold are discarded, and the rest of crosscorrelations, with values above the threshold, are included in the spectra computation. Therefore, we sum only crosscorrelations whose contribution have comparatively larger associated significance values. One might choose, for instance, to include in the summation only a relatively small percentage (e.g., 30%) of all possible crosscorrelations — those with the most resolving power.

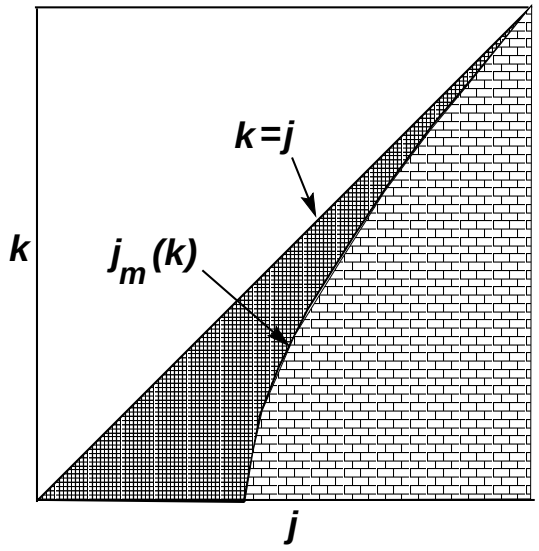

Figure 1. Cartoon indicating those combinations of traces j and k whose crosscorrelations are used in the selective-correlation-sum method (shown as the brick pattern) and those combinations that are excluded from the sum (shown as the fine rectangular-grid pattern).

Figure 1 depicts the idea. The ordinate in the figure represents trace number k, and the abscissa trace number j for trace pairs that might be crosscorrelated. Ignore the triangular region shown in white because we consider only $k < j$. The region shown by the brick pattern of shading depicts those combinations of trace indices k and j for which crosscorrelations are included in the velocity-analysis computation. The region shaded in a fine rectangular pattern depicts those crosscorrelations that are excluded from the sum. Thus, in the selected-correlation-sum approach, equation (1) is modified to

$$UC_{sc}(v_{trial}, t_0) = \sum_{k=1}^{M-d_m} \sum_{j=k+d(k)}^{M} \sum_{w} f_{k,t(k)}\ f_{j,t(j)}. \tag{5}$$

The changes from equation (1) to equation (5) are solely in the lower limit for the sum over j and the upper limit for the sum over k. Here, $d(k)$ is the minimum difference $j-k$, which is a function of k, and d_m is the minimum of $d(k)$ for all k. As depicted in Figure 1, $d(k)$ will always be a monotonically decreasing function of k.

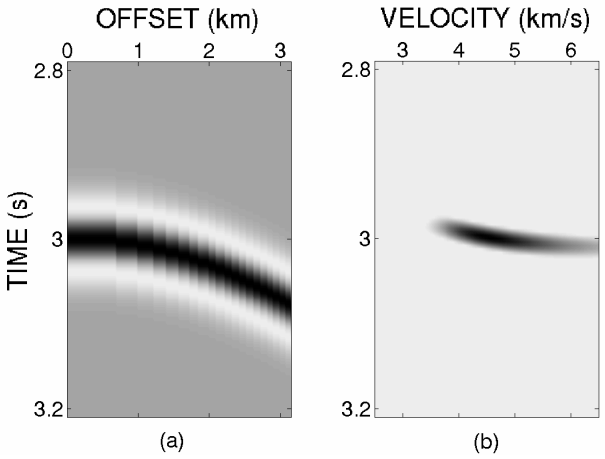

Figure 2. (a) Synthetic CMP gather with a reflection single event; (b) velocity panel for the synthetic data. The broad region of large spectral amplitude indicates potential for large uncertainty in picking stacking velocity.

This process should improve the velocity resolution of the spectra-computation process and thus possibly reduce uncertainty in the velocity picking. Moreover, it could result in a better separation between the maxima of closely interfering reflections and could reveal the maximum of a weak primary submerged along the flank of the coherence peak of a strong multiple.

Next we illustrate, first with noise-free synthetic data, how the selective-correlation sum process alters the resolution of velocity estimation when it is applied to velocity-spectra calculation. We then demonstrate, also on synthetic data, the relative robustness of this method and conventional velocity analysis for estimating primary stacking velocity in the presence of contaminating factors such as additive noise, statics time distortions, and nearby primaries and multiples.

Tests on noise-free synthetic data

The first model consists of a single horizontal reflector below a homogeneous layer with velocity of 4.5 km/s and layer thickness of 6.75 km. Figure 2a shows a CMP gather with cable length 3150 m, receiver group interval 50 m, and Ricker wavelet with peak frequency 12.5 Hz, and Figure 2b shows the corresponding velocity panel computed with the conventional unnormalized crosscorrelation sum, which uses the crosscorrelations of all possible trace pairs. Note the spread of strong spectral amplitude across the velocity panel, extending from 3.5 km/s all the way to the right side of the velocity panel at 6.5 km/s. The smearing here is the result of a combination factors: relatively low frequency, high velocity, and large reflector depth. This smearing suggests large uncertainty in the velocity picking. Figure 3a is the same velocity panel shown in Figure 2b with 100% of the crosscorrelations included. (Henceforth, 100% of crosscorrelations means the conventional crosscorrelation sum, with all crosscorrelations included in the sum. Any reduced percentage means that the approach of selective-crosscorrelation sum is used, and the specified percentage is the percentage of all possible crosscorrelations that are used in the sum.) The plots in Figure 3 are velocity spectra computed using 50% of all possible crosscorrelations (Figure 3b), 25% (Figure 3c), and 10% (Figure 3d). Apparent resolution in picking a velocity for the reflection event of Figure 2a is improved with decreasing percentage of crosscorrelations summed.

In order to more closely assess the results, in Figure 4 are plots of coherence curves — plots of UC_{sc} as a function of trial velocity v_{trial} for normal-incidence time t_0 equal to that of the reflection of interest. Shown in Figure 4 are coherence curves at $t_0 = 3$ s, extracted from Figure 3 (each curve is normalized to a peak amplitude of unity). As expected, lowering the percentage of crosscorrelations used in the selective sum results in a sharpening of the peak of the coherence curve.

This improvement in velocity resolution should aid in interpretation of closely interfering events, such as primaries and multiples. Figure 5a shows a CMP gather containing two events with the same zero-offset arrival time of 2 s, but with different stacking velocities of 4.5 km/s and 3.5 km/s. At offsets larger than 2 km, the difference in NMO of the two events is observable. In this example, the peak frequency of the Ricker wavelet in the data is again 12.5 Hz. Figure 5b shows the velocity panel for these data, computed using the conventional crosscorrelation-sum method. From study of the velocity panel it is impossible to distinguish the two events present in the data; the most probable pick would be around a velocity of 4 km/s. The selective-crosscorrelation sum allows separation of the two maxima, yielding good estimates of the velocity of each reflection (Figure 6b). The coherence curves for zero-offset time of 2 s, in Figure 7, reveal the substantial improvement in resolution when the 25% of the crosscorrelations with largest associated differential moveouts are used in the sum. Based on a number of similar tests, significant improvement is achieved for percentages of 50% or less.

Another coherence measure commonly used in velocity analysis is conventional semblance, described by Neidell and Taner (1971). The conventional semblance, also called *semblance coefficient* SC, is the normalized coherence measure given by

$$SC(v_{trial}, t_0) = \frac{\sum_w \left\{ \sum_{j=1}^{M} f_{j,t(j)} \right\}^2}{M \sum_w \sum_{j=1}^{M} f_{j,t(j)}^2}. \qquad (6)$$

According to resolution tests made by Neidell and Taner (1971), with a noise-free synthetic data set the semblance performed better than the unnormalized crosscorrelation sum. The coherence curves in Figure 8 confirm this result, but also demonstrate that the difference

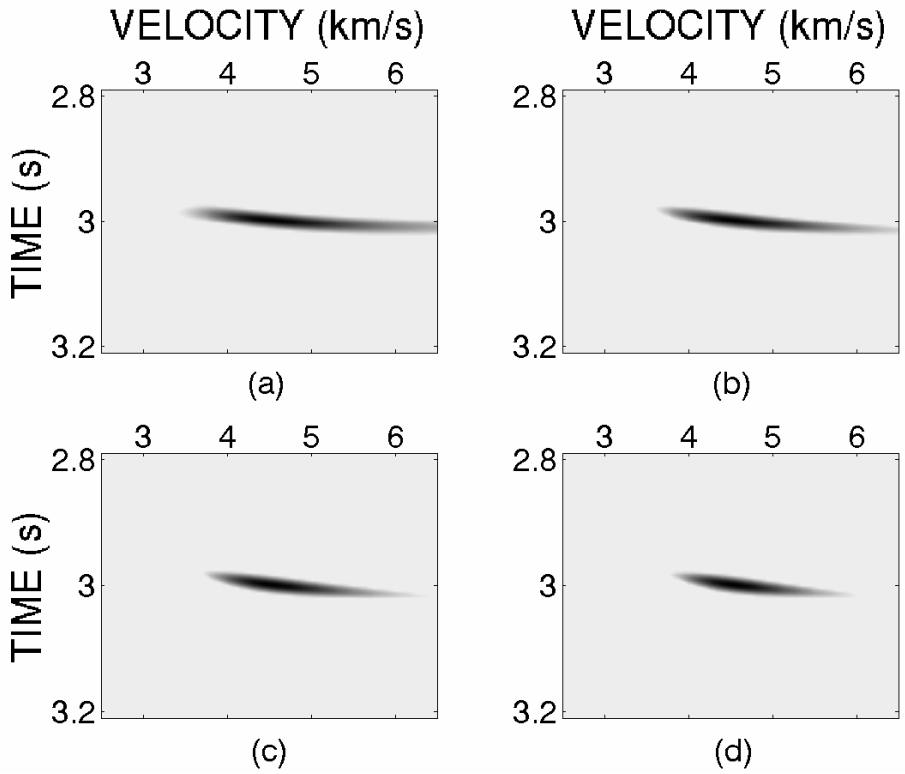

Figure 3. Velocity panels computed using: (a) conventional crosscorrelation sum (100% of crosscorrelations included) and using selective-correlation sum with the percentages (b) 50%, (c) 25%, and (d) 10%.

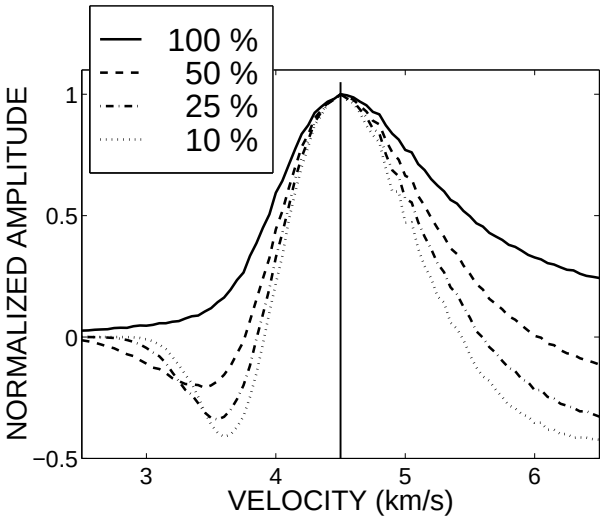

Figure 4. Coherence curves for the conventional crosscorrelation sum (100%), and selective-correlation sum for the percentages 50%, 25%, and 10%. The vertical line indicates the correct stacking velocity.

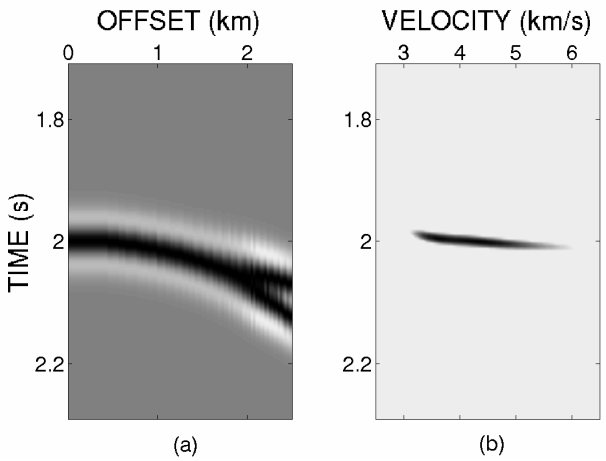

Figure 5. (a) Synthetic gather with two interfering events, and (b) velocity panel for the data. From this velocity panel, it is impossible to identify the presence of two events.

in performance is small, particularly in comparison with the improvement in velocity resolution achieved by using selective-correlation sum.

Another way to increase velocity resolution is through use of optimum trace weights such as those produced by Schoenberger's multiple-suppression method. In his method, a weight is assigned to each data trace, prior stacking, based on least-squares optimization.

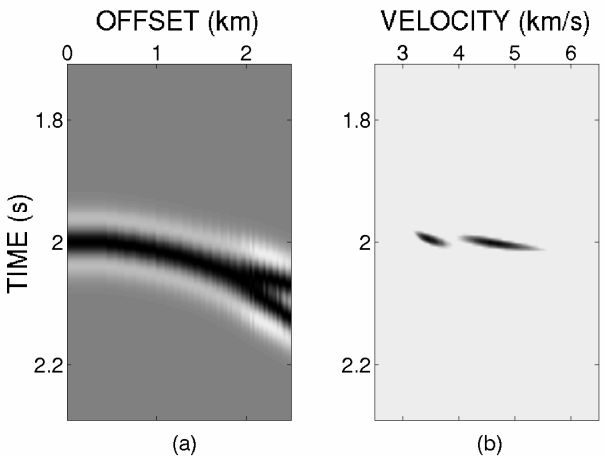

Figure 6. (a) Same CMP gather as in Figure 5; (b) velocity panel computed using selective-correlation sum with a 25% of crosscorrelations

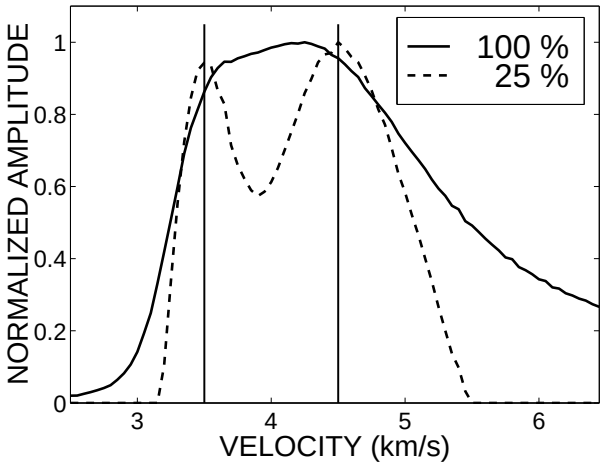

Figure 7. Coherence curves for two interfering events. Conventional crosscorrelation sum (100%) and selective-correlation sum (25%). The vertical lines indicate the correct velocities for the two events.

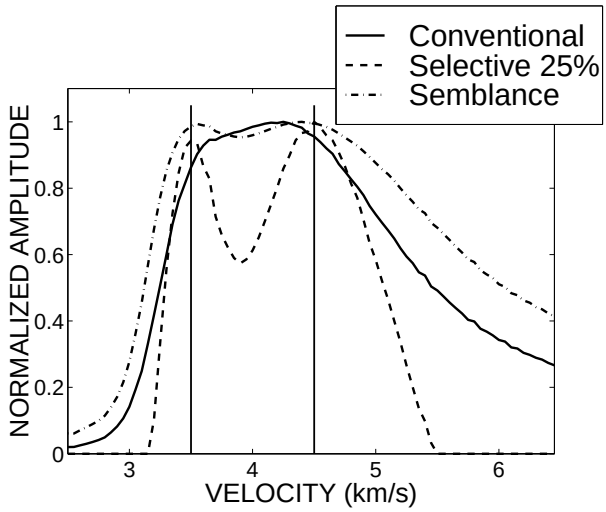

Figure 8. Coherence curves for two interfering events using conventional crosscorrelation sum, selective-correlation sum (25%), and semblance. The vertical lines indicate the correct velocities for the two events.

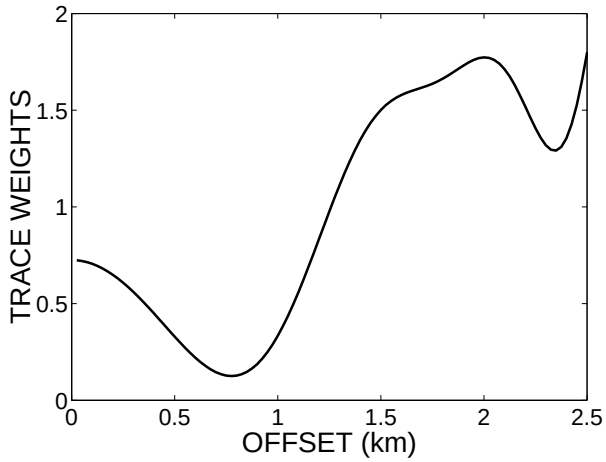

Figure 9. Optimum stacking weights used prior to conventional velocity estimation for the synthetic CMP gather with interfering events, shown in Figure 5a.

CMP stacking with these weights constitutes a stacking filter designed to reject multiples, based on their frequency content and residual moveout, after data have been NMO-corrected to align primaries. This generally results in better multiple attenuation than does the conventional stack, in which traces are weighted equally. For our purpose of improving velocity resolution, the weights produced in Schoenberger's method are applied directly to the traces in the CMP gather prior to performing conventional velocity analysis.

The weights designed for optimum rejection of one of the interfering events plotted in Figure 5a, and preservation of the other, are shown in Figure 9. As seen in this figure, the procedure gives relatively more importance to long-offset traces than to short- and intermediate-offset ones. Applying the weights to the traces in the CMP gather of Figure 5a, and then performing velocity analysis using conventional crosscorrelation sum, produced the coherence curve shown as the dashed line in Figure 10. The solid line pertains to the conventional velocity-analysis method applied to traces with uniform weights. Indeed, with the use of optimum weights, resolution is improved when compared with that of either the conventional crosscorrelation sum or the semblance coefficient (Figure 8), but still the selective-correlation sum (Figures 7 and 8) performs better in separating the two maxima. (Note also the slight error in velocities as-

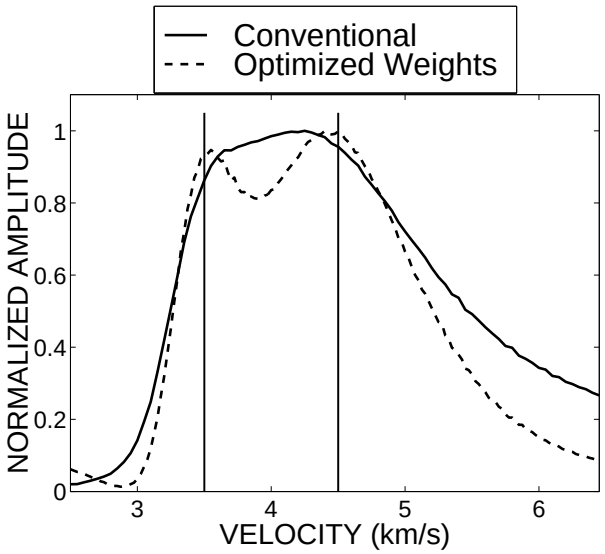

Figure 10. Coherence curves, for conventional crosscorrelation sum with use of uniform and optimum weights, for the interfering-event data. The vertical lines indicate the correct velocities.

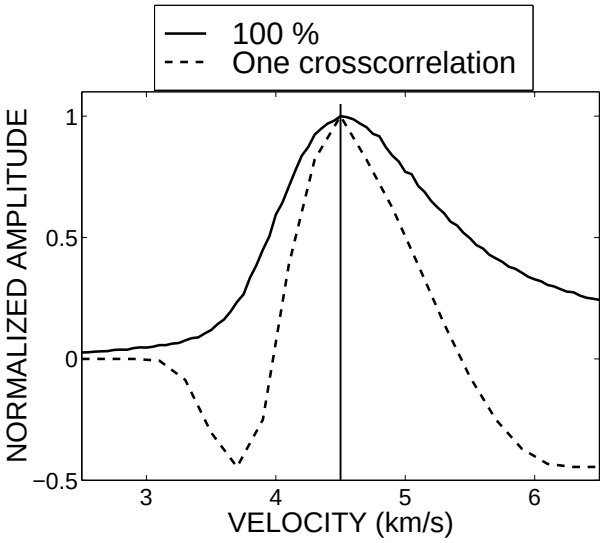

Figure 11. Conventional crosscorrelation sum (100%) for same data of Figure 2, and selective-correlation sum including only the single crosscorrelation with the largest differential moveout in the CMP gather.

sociated with the peaks in the dashed coherence curve in Figure 10.)

Because the weights are optimized for a specific set of problem parameters, the result for optimum weights is fixed by the weights used, whereas selective-correlation sum provides one with a knob that can be fully opened (100% of crosscorrelations, equivalent to conventional crosscorrelation sum) or closed until a desired percentage of crosscorrelations is reached (e.g., 50%, 25%). Aside from a scale-factor change in the coherence curves, the difference as the knob is turned is that the lower the percentage used, the higher the resolution.

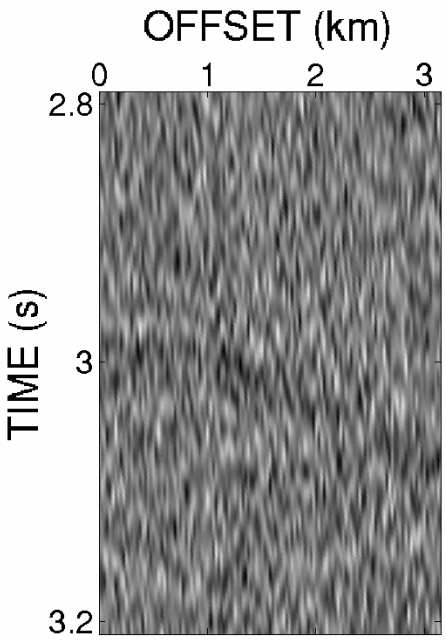

Figure 12. CMP gather with the same single reflection event as in Figure 2, with bandlimited random noise added such that SNR = 0.5.

In principle, one could go from including all crosscorrelations to the extreme of including only one, that being the correlation between the shortest and the longest offset traces. Figure 11 shows coherence curves for these upper and lower extremes in velocity estimation for the same data of Figure 2. The solid line corresponds to the coherence curve of conventional crosscorrelation sum, that is 100% of crosscorrelations included, and the dashed one to the selective-correlation sum including only the single crosscorrelation for the traces with the largest differential moveout in the CMP gather. The peaks of the two curves coincide at the correct velocity, implying that, in absence of noise (which, unfortunately, is ubiquitous), one could estimate velocity using just the first and last trace of the CMP data. Below, we will see that when the velocity at the peak is in error because of either statics distortions or additive noise, the error is quite independent of the percentage used in the selective-sum.

Noise-contaminated synthetic data

The sharpening of the peak in coherence curves does not itself mean a reduction in uncertainty in picking stack-

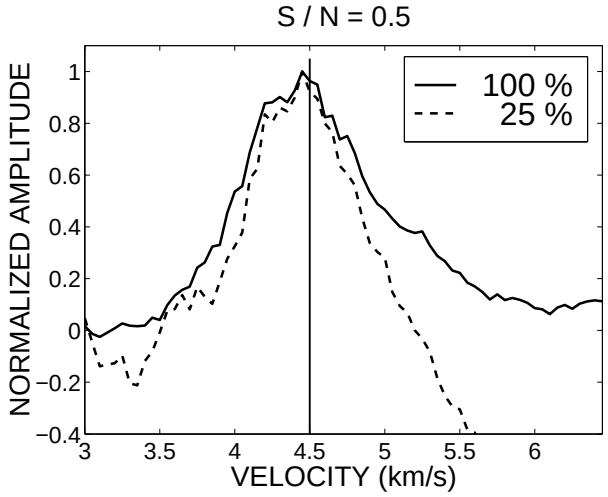

Figure 13. Coherence curves, for data with SNR = 0.5, using conventional crosscorrelation sum (100%) and selective-correlation sum (25%). The vertical line indicates the correct velocity.

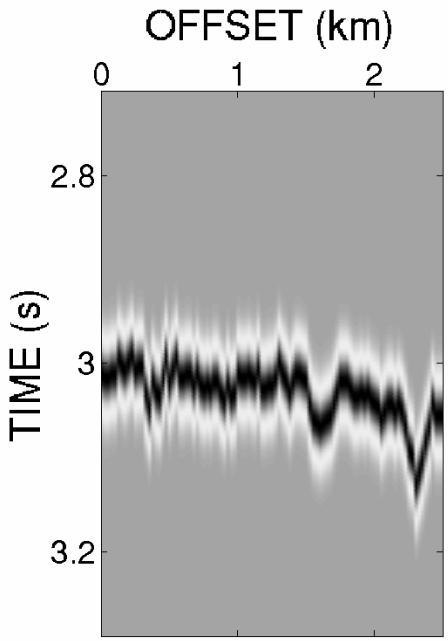

Figure 14. Synthetic CMP gather containing a reflection at t_0 = 3 s, with random static time distortions (standard deviation = 80 ms) applied.

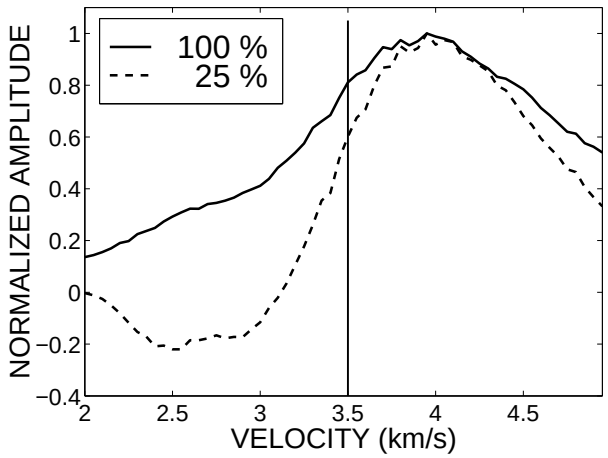

Figure 15. Coherence curves, for the event in Figure 14, computed using conventional crosscorrelation sum (100%) and selective-correlation sum (25%).

ing velocity. Of comparable importance is the performance of any chosen coherency method in the presence of contaminating factors such as additive noise, static time anomalies, and strong multiples. Let us next consider data contaminated by additive noise.

Here, the signal-to-noise ratio (SNR) is computed as the ratio of the peak amplitude of the reflection signal to the root-mean-squared (rms) amplitude of the noise. Figure 12 shows a single-event CMP gather with uncorrelated, random noise bandlimited to the same passband as the signal. In these data, SNR = 0.5. The reflector model and data parameters in this example are the same as those in Figure 2. Figure 13 shows the corresponding coherence curves for conventional crosscorrelation sum (solid line), and selective-correlation sum using 25% of the crosscorrelations (dashed line). We make two observations. First, for the selective-correlation sum, the peak of the curve is again sharper than that of the curve for conventional crosscorrelation sum, implying higher resolution; second, both peaks are located at about the same velocity (which is not necessarily the correct one), suggesting that accuracy of both methods is comparable. In numerous tests, we have observed that the peaks in the curves for both methods coincide when the percentage used in the sum is not too small (say, 20% or higher). Moreover, the location of the velocity peak is governed strongly by crosscorrelations for pairs of traces with large differential moveout. Because the selective-correlation method includes trace pairs that have relatively large differential moveout, it includes those trace pairs that dominate the contributions in conventional velocity analysis, supporting our observation that the robustness of the selective-correlation-sum method in the presence of uncorrelated noise is comparable to that of conventional velocity analysis.

Statics-contaminated synthetic data

Another source of errors in velocity estimation is static time distortions. In the next example, we consider a CMP gather with a reflection event containing static distortions (Gaussian random) with a large standard

deviation of 80 ms (Figure 14). A 5-point lateral running average was applied to the random sequence of time distortions to introduce lateral correlation in the simulated statics. The model for this example is a single horizontal reflector below a homogeneous layer with velocity of 3.5 km/s and layer thickness of 5.25 km, and the cable length is 3150 m, group interval is 25 m, and peak Ricker-wavelet frequency is 12.5 Hz. Figure 15 shows the coherence curves for the statics-distorted reflection, again using conventional crosscorrelation sum (solid line), and selective-correlation sum (dashed line) for 25% of crosscorrelations.

For these data, normal moveout (NMO) is relatively small, making it comparable to the size of statics distortions. As shown in Figure 15, peaks in the coherence curves are biased toward velocities that, for this realization of statics, are about 500 m/s higher than the correct velocity. Note, however, that the peaks of the coherence curves computed using both the conventional and selective-correlation method coincide, but at this wrong velocity value. For this extreme example of static distortions, selective-correlation sum has improved velocity resolution over that of the conventional crosscorrelation sum, and has done so with comparable (in)accuracy. As with the error in velocity picking in the presence of data contamination by additive noise, picking errors introduced by static time distortions are independent of the percentage used in the selective-correlation-sum method for percentages that exceed about 20%.

Strong multiples

In conventional velocity estimation, strong-amplitude multiples can swamp nearby primaries with amplitudes that are weaker than those of the multiples. Figure 16 shows three CMP gathers, each with four reflections and associated multiples. The ratio shown beneath each CMP gather is the ratio of the amplitude of primary to that of multiple. The CMP gather on the left has primaries and multiples with the same strength. For the gather in the middle, the amplitude of multiples is twice of that of primaries, and for the gather on the right, multiples amplitudes are three times those of primaries. The corresponding velocity spectra for the CMP gathers of Figure 16, using conventional crosscorrelation sum, are shown in Figure 17 and, using selective-correlation sum for 25% of crosscorrelations, are shown in Figure 18. Selective-correlation sum separates primaries and multiples even when the amplitude of the multiple is much stronger than that of primaries, allowing easier interpretation of primary stacking velocities. The conventional correlation sum (Figure 17) is so dominated by the multiples when their amplitudes are stronger than those of primaries that no peak may be identified for some primaries. Even when amplitudes of primaries and multiples are equal, no separation is evident on the deeper events.

Synthetic gather with many reflections

Not only can multiples interfere with primaries, closely-arriving primary reflections can sometimes confuse velocity spectra, particularly for low-fold data. Bringing a bit more realism into our synthetic data examples, we have generated a synthetic CMP gather with many hyperbolic reflection events.

We generated a random series of 18 primary reflections and nine multiples (both with Poisson distribution of arrival times) for the one-dimensional velocity model of Figure 19. The solid line is the interval velocity function used to derive rms velocities for the modeling of the primary events, and the dashed one is the interval-velocity function used to generate the multiples. Figure 20a shows a synthetic CMP gather with spreadlength of 2 km, group interval of 25 m, Ricker wavelet peak frequency of 12.5 Hz, and SNR of about 2. For these 80-fold CMP data, the total number of crosscorrelations performed in the calculation of the spectrum, for fixed trial velocity and normal-incidence two-way time, is 3160. The corresponding velocity spectra computed using conventional crosscorrelation sum is shown in Figure 20b. The dash-dot line shows the rms velocity of the multiples, and the dashed line shows that of the primaries. Note, as in examples above, the spreading of the coherence functions, making difficult the correct identification of peaks with primary velocities.

Only 790 crosscorrelations are included in the sum when 25% is chosen in the selective-correlation velocity analysis for these CMP data. The velocity panel computed applying selective-correlation sum for these data is shown in Figure 21b. Considerably higher resolution is achieved in the results of selective-correlation sum. The trend of primary velocity function is better identified in Figure 21b than in Figure 21b.

Another way to reduce the number of crosscorrelations to 25% of the original is simply to halve the fold of the data by dropping every other trace from the CMP gather, thereby doubling the group interval. This action, however, by no means increases the resolution of stacking velocity. The CMP gather shown in Figure 22a is the same as that of Figure 20a, but with fold reduced from 80 to 40. Thus, the total number of crosscorrelations in conventional crosscorrelation sum (i.e., with no deletion of crosscorrelations based on differential moveout) for these CMP data is the same (790) as when we applied selective-correlation sum using 25% of crosscorrelations for the 80-fold data. Figure 22b shows the velocity panel for the reduced-fold data using conventional crosscorrelation sum. Reducing fold and performing conventional velocity analysis does not increase velocity resolution and also has little influence on the character of the velocity spectra (compare Figures 20b and 23b). If fold becomes too small as a result of increasing the group interval, however, one can expect extraneous peaks (artifacts) in the velocity spectra.

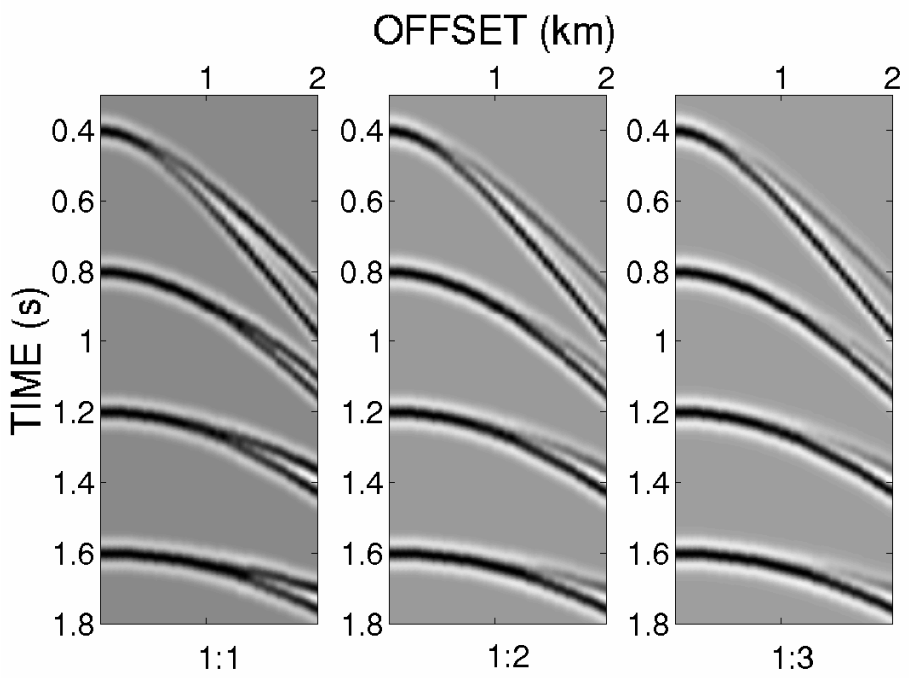

Figure 16. Synthetic CMP gathers with different ratios of primary-to-multiple amplitude.

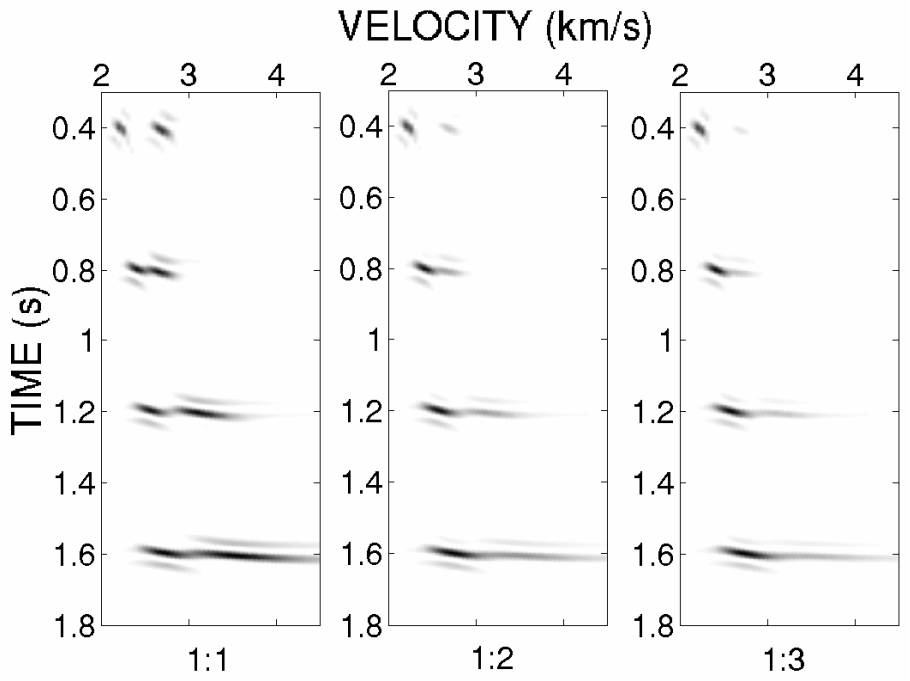

Figure 17. Velocity panels, for different ratios of primary-to-multiple amplitude, using conventional crosscorrelation sum.

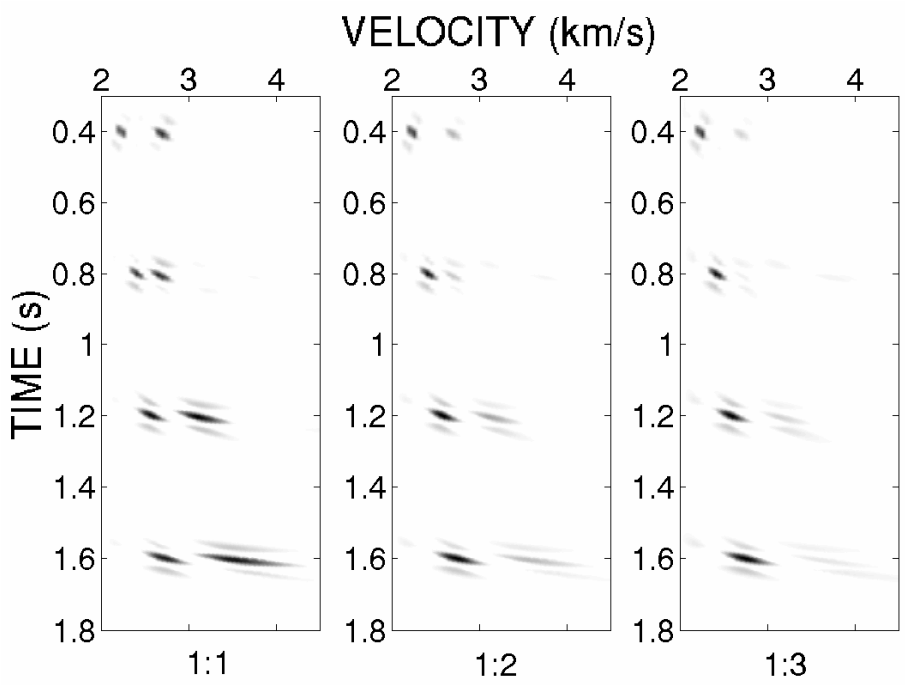

Figure 18. Velocity panels, for different ratios of primary-to-multiple amplitude, using selective-correlation sum (25%).

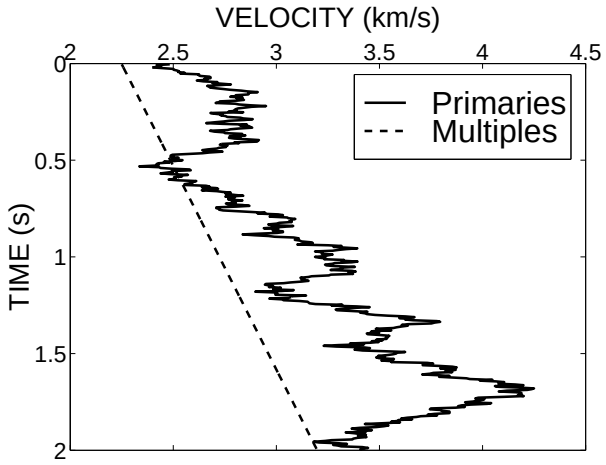

Figure 19. One-dimensional velocity model for primaries (solid line) and multiples (dashed line).

Computational effort

The unnormalized crosscorrelation sum UC [expression (1)], can be written as an energy difference:

$$UC(v_{trial}, t_0) = \frac{1}{2} \sum_w \left\{ \left\{ \sum_{j=1}^{M} f_{j,t(j)} \right\}^2 - \sum_{j=1}^{M} f_{j,t(j)}^2 \right\}. \quad (7)$$

Expression (7) is a convenient and commonly-implemented form of this coherence measure because of the relatively small number of operations involved (order MN, where M is the number of traces in the CMP gather, and N is the number of samples in the time window w), whereas expression (1) seems to need order M^2N multiplications. The energy-difference form in equation (7), however, does not lend itself to selectively deleting some of the crosscorrelations from the sum. Fortunately, expression (1) need not require order M^2N multiplications. It can be simply rewritten as

$$UC(v_{trial}, t_0) = \sum_w \sum_{k=1}^{M-1} f_{k,t(k)} \left\{ \sum_{j=k+1}^{M} f_{j,t(j)} \right\}. \quad (8)$$

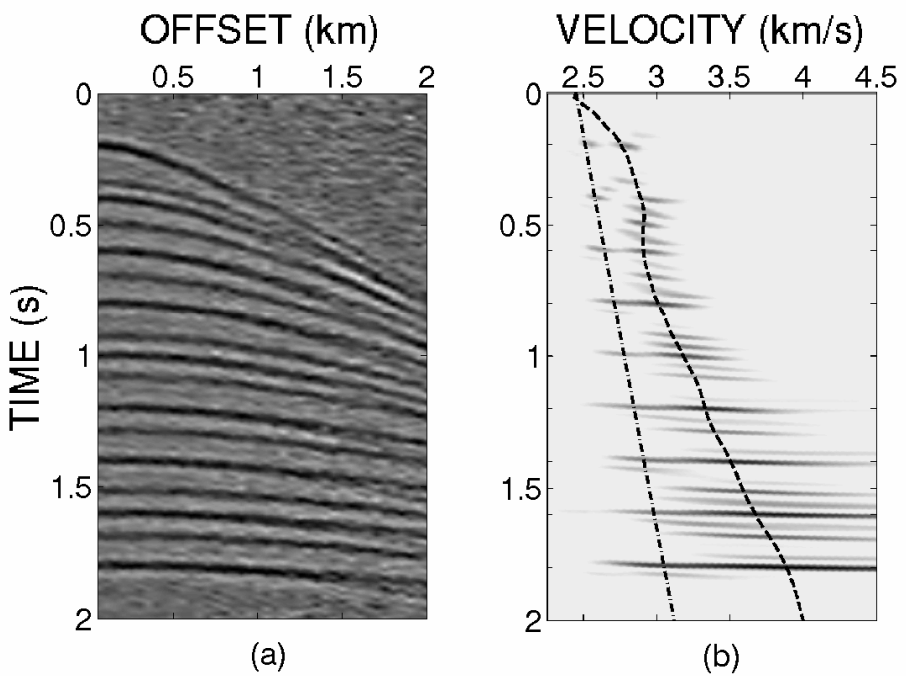

Figure 20. (a) CMP gather with many reflections; (b) conventional crosscorrelation sum. The dashed line represents the rms velocity of the primaries, and the dash-dot line that of the multiples.

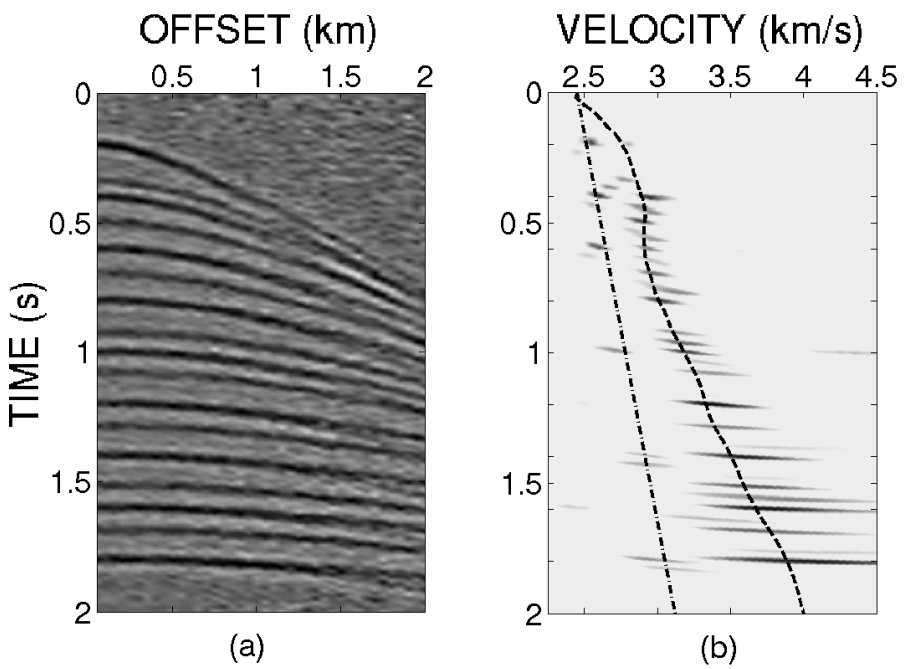

Figure 21. (a) CMP gather with many reflections; (b) selective-correlation sum with 25% of crosscorrelations summed. The dashed line represents the rms velocity of the primaries, and the dash-dot line that of the multiples.

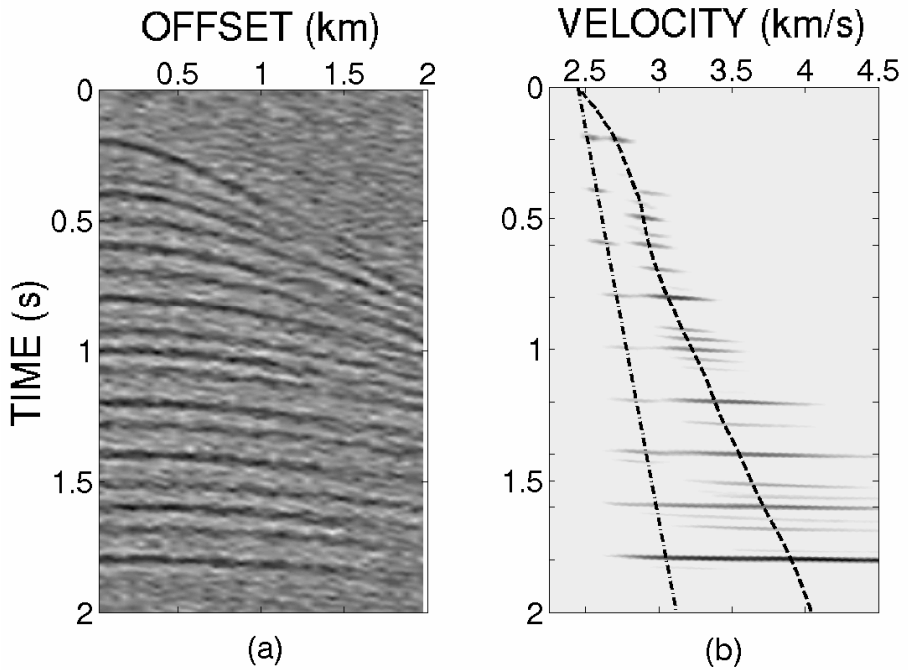

Figure 22. (a) Same CMP data as in Figure 19a with fold reduced from 80 to 40; (b) conventional crosscorrelation sum for the data with reduced fold.

In this form, as traces are read into memory they are multiplied with an accumulating sum of traces that had previously been read into memory. The number of computations in this form is just order MN.

Selective-correlation sum can be implemented in much the same way. Specifically, equation (5) can be rewritten in the same manner as was done for equation (8), giving

$$UC_{sc}(v_{trial}, t_0) = \sum_{w} \sum_{k=1}^{M-d_m} f_{k,t(k)} \left\{ \sum_{j=k+d(k)}^{M} f_{j,t(j)} \right\}. \quad (9)$$

With this expression, the selective-correlation-sum method also requires only order MN computations, making it comparable in computation cost to that of conventional velocity analysis. The only added burden caused by selectively deleting crosscorrelations is a requirement for more random-access memory, but the added memory requirement is insignificant.

Discussion

By including in the sum of crosscorrelations used in velocity analysis only those correlations with the relatively high resolving power, one can increase velocity resolution for data with both isolated and interfering events, including data contaminated with multiple reflections, added Gaussian noise, and static time distortions.

We compared results of the selective-correlation-sum method with those of several other methods for computing velocity spectra: conventional crosscorrelation sum, semblance coefficient, and conventional crosscorrelation sum using trace weights designed for optimum enhancement of primary-to-multiple ratio in CMP stacking. In all tests, for percentages of crosscorrelations 50% or less, selective-correlation sum yielded improved velocity resolution relative to that achieved by the other methods. Selective-correlation sum provides a new parameter — the percentage of crosscorrelations included in the sum — that controls a tradeoff between increasing resolution and effectiveness in attenuating random noise.

Tests on synthetic data show that, in the presence of static distortions and additive random noise, selective-correlation velocity analysis has accuracy for estimating the stacking velocity that is comparable to that of conventional crosscorrelation sum. An interesting observation in our tests is that the error that statics time distortions and random noise introduce in picked stacking velocity is quite independent of the percentage used in the selective-correlation method, for percentages from about 20% up to 100%. The peak in velocity spectra for both selective-correlation velocity analysis and conventional velocity analysis is determined largely by crosscorrelations of trace pairs with relative large differential moveout.

The implementation of selective-correlation sum described here entails only a simple modification of con-

ventional velocity analysis and thus achieves its increase in velocity resolution at computational cost that is comparable to that of conventional velocity analysis.

Acknowledgments

The authors especially thank PDVSA-Intevep for its funding support of Valmore Celis's graduate studies at Colorado School of Mines.

REFERENCES

Biondi, B. L., and Kostov, C., 1989, High resolution velocity spectra using eigenstructure methods: Geophysics, **54**, 832-842.

De Vries, D., and Berkhout, A. J., 1984, Velocity analysis based on minimum entropy: Geophysics, **49**, 2132-2142.

Gelchinsky, B., Landa, E., and Shtivelman, V., 1985, Algorithms of phase and group correlation: Geophysics, **50**, 596-608.

Key, S. C., and Smithson, S. B., 1990, New approach to seismic-reflection event detection and velocity determination: Geophysics, **55**, 1057-1069.

Kirling, R. L., Dewey, L. A., Bradley, J. N, 1984, Optimum seismic velocity estimators: Geophysics, **49**, 1861-1868.

Neidell, N. S., and Taner, M. T., 1971, Semblance and other coherency measures for multichannel data: Geophysics, **36**, 498-509.

Schoenberger, M., 1996, Optimum weighted stack for multiple suppression: Geophysics, **61**, 891-901.

Sherwood, J. W., and Poe, P. H., 1972, Continuous velocity estimation and seismic wavelet processing: Geophysics, **37**, 769-787.

Taner, M. T., and Koehler, F., 1969, Velocity spectra: digital computer derivation and applications of velocity functions, **34**, 859-881.

Toldi, J. L., 1989, Velocity analysis without picking: Geophysics, **54**, 191-199.